

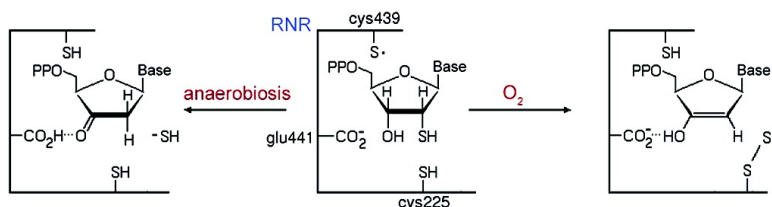
Article

## Theoretical Study on the Inhibition of Ribonucleotide Reductase by 2'-Mercapto-2'-deoxyribonucleoside-5'-diphosphates

Susana Pereira, Pedro Alexandrino Fernandes, and Maria Joo Ramos

*J. Am. Chem. Soc.*, **2005**, 127 (14), 5174-5179 • DOI: 10.1021/ja046662w • Publication Date (Web): 18 March 2005

Downloaded from <http://pubs.acs.org> on March 25, 2009



### More About This Article

Additional resources and features associated with this article are available within the HTML version:

- Supporting Information
- Links to the 2 articles that cite this article, as of the time of this article download
- Access to high resolution figures
- Links to articles and content related to this article
- Copyright permission to reproduce figures and/or text from this article

[View the Full Text HTML](#)

## Theoretical Study on the Inhibition of Ribonucleotide Reductase by 2'-Mercapto-2'-deoxyribonucleoside-5'-diphosphates

Susana Pereira, Pedro Alexandrino Fernandes, and Maria João Ramos\*

Contribution from REQUIMTE, Departamento de Química, Faculdade de Ciências do Porto, Rua do Campo Alegre, 687, 4169-007 Porto, Portugal

Received June 7, 2004; E-mail: mjramos@fc.up.pt

**Abstract:** Ribonucleotide reductase (RNR) is responsible for the reduction of ribonucleotides into the correspondent 2'-deoxyribonucleotides in the only physiological process that yields the monomers of DNA. The enzyme has thus become an attractive target for chemotherapies that fight proliferation-based diseases, specifically cancer and infections by some viruses and parasites. 2'-Mercapto-2'-deoxyribonucleoside-5'-diphosphates (SHdNDP) are mechanism-based inhibitors of RNR and therefore potential chemotherapeutic agents for those indications. Previous experimental studies established the in vitro and in vivo activity of SHdNDP. In the in vitro studies, it was observed that the activity was dependent on the oxidative status of the medium, with the inactivation of RNR only occurring when molecular oxygen was available. To better understand the mechanism involved in RNR inactivation by SHdNDP, we performed theoretical calculations on the possible reactions between the inhibitors and the RNR active site. As a result, we propose the possible mechanistic pathways for the chemical events that occur in the absence and in the presence of O<sub>2</sub>. They correspond to a refinement and a complement of those proposed in the literature.

### Introduction

Ribonucleotide reductase (RNR) catalyzes the reduction of ribonucleotides into the correspondent 2'-deoxyribonucleotides, in the rate-limiting step for the synthesis of DNA monomers. It is a highly regulated enzyme, with a cell cycle-dependent activity that ensures the maintenance of a permanently low cellular pool of deoxyribonucleotides. DNA replication, which must occur prior to each cell division, is therefore greatly dependent on the activity of RNR. The same stands for the reverse transcription of viral RNA in retroviral infections. As such, RNR became a very important element in the effort to control proliferation-based diseases, and, in the last years, several molecules that are able to impair RNR activity have been applied effectively in anti-cancer, anti-viral, and anti-parasite therapies.<sup>1-5</sup>

Life on earth is believed to have been RNA-based at the very beginning. Nowadays, with the exception of viroids and virusoids, all modern organisms have their genetic information encoded in a DNA molecule, and all need an RNR enzyme that transforms the RNA monomers into the DNA ones.<sup>6</sup> Different organisms have related RNRs; for instance, their catalytic mechanism is always based on radical-mediated reactions.<sup>7</sup> The

main evolutionary differences lie in the cofactor needed to produce the essential organic radical, the active site residues that perform catalysis, and the phosphorylation state of the substrates. In mammalian RNR (class Ia), the essential radical is located in a tyrosine residue, generated and stabilized by an adjacent oxygen-linked non-heme iron cluster, and the active site residues directly involved in the reduction are three cysteines, a glutamate, and an asparagine. The substrates of this RNR are ribonucleoside-5'-diphosphates.

The *Escherichia coli* RNR is similar to the mammalian and has served as its prototype in experimental studies. The determination of its crystallographic structure was a step forward in the unraveling of the catalytic mechanism and in the development of new inhibitors.<sup>8</sup> *E. coli* RNR is constituted by two different homodimeric subunits. The larger one, known as R1, lodges the active site and the binding sites for the allosteric regulators; the smaller, known as R2, harbors the iron cluster and the organic free radical, located in Tyr<sub>122</sub>. The active site residues that are catalytically important are Cys<sub>225</sub>, Cys<sub>439</sub>, Cys<sub>462</sub>, Glu<sub>441</sub>,<sup>9</sup> and Asn<sub>437</sub>.<sup>10</sup> For catalysis to begin, the tyrosyl radical in R2 must generate a thiyl one in Cys<sub>439</sub> of the active site in R1. This is thought to occur by proton-coupled electron transfers, through a ca. 35 Å long chain of hydrogen-bonded residues. A generally accepted proposal for RNR catalytic mechanism is presented in Scheme 1.<sup>7</sup>

(1) Murren, J.; Modiano, M.; Clairmont, C.; Lambert, P.; Savaraj, N.; Doyle, T.; Sznol, M. *Clin. Cancer Res.* **2003**, *9*, 4092.

(2) Lee, Y.; Vassilakos, A.; Feng, N. P.; Lam, V.; Xie, H. S.; Wang, M.; Jin, H. N.; Xiong, K. Y.; Liu, C. Y.; Wright, J.; Young, A. P. *Cancer Res.* **2003**, *63*, 2802.

(3) Heinemann, V. *Oncology* **2003**, *64*, 191.

(4) Mayhew, C. N.; Mampuru, L. J.; Chendil, D.; Ahmed, M. M.; Phillips, J. D.; Greenberg, R. N.; Elford, H. L. *Antiviral Res.* **2002**, *56*, 167.

(5) Ingram, G. M.; Kinnaird, J. H. *Parasitol. Today* **1999**, *15*, 338.

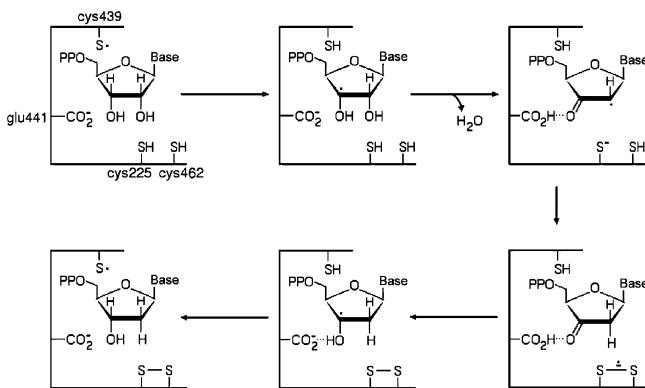
(6) Reichard, P. *Science* **1993**, *260*, 1773.

(7) Stubbe, J.; van der Donk, W. A. *Chem. Rev.* **1998**, *98*, 705.

(8) Eriksson, M.; Uhlin, U.; Ramaswamy, S.; Ekberg, M.; Regnstrom, K.; Sjöberg, B.-M.; Eklund, H. *Structure* **1997**, *5*, 1077.

(9) Persson, A. L.; Eriksson, M.; Katterle, B.; Pötsh, S.; Sahlin, M.; Sjöberg, B.-M. *J. Biol. Chem.* **1997**, *272*, 31533.

(10) Kasrayan, A.; Persson, A. L.; Sahlin, M.; Sjöberg, B.-M. *J. Biol. Chem.* **2002**, *277*, 5749.

**Scheme 1.** Mechanism of Ribonucleotide Reduction by RNR

In the first step, the 3'-H atom is abstracted by the radical sulfur of Cys<sub>439</sub>.<sup>11,12</sup> After protonation of the 2'-OH group by Cys<sub>225</sub> and loss of a water molecule,<sup>13,14</sup> Cys<sub>225</sub> and Cys<sub>462</sub> reduce the ribose and become oxidized to a disulfide bridge.<sup>7</sup> With the spin density replaced in C3', the final step consists of the donation of the hydrogen atom by Cys<sub>439</sub> back to that carbon. Thus, the 2'-deoxyribonucleotide is formed and the essential tyrosyl radical is regenerated.<sup>11</sup>

Several modifications of the nucleotides' ribose moiety at the 2'-position have produced potent mechanism-based inhibitors of RNR.<sup>15–18</sup> 2'-Mercapto-2'-deoxyribonucleoside-5'-diphosphates (SHdNDP) are included among them. The uridine analogue (SHdUDP) inhibits the purified RNR of *E. coli* very efficiently,<sup>19</sup> and the cytidine analogue was found to be the most effective in lowering the deoxynucleotide levels and the proliferation of the human lymphoblastoid cell line CEM/SS, probably due to a more efficient phosphorylation inside the cells.<sup>20</sup> The *in vitro* studies with SHdUDP revealed specific features in the reaction mechanism, which suggest a different behavior if compared to similar compounds.<sup>19</sup> RNR inhibition only occurred if the experiment took place in the presence of molecular oxygen. In this situation, subunit R2 was specifically targeted through irreversible scavenging of the essential tyrosyl radical. The role of R1 in RNR activity was not affected. The transient formation of an unstable radical was detected. From the analysis of its EPR spectrum and the results of mutagenic and isotopic labeling studies, it was suggested to be a perthiyl radical located in an active site cysteine, probably Cys<sub>225</sub>. When the experiment was carried out in anaerobic conditions, the enzyme remained active, the tyrosyl radical was not lost, and the transient radical was not formed, suggesting that the reaction proceeded as with the normal substrate.

This work consists of a theoretical study of the interaction between 2'-mercapto-2'-deoxyribonucleotides and RNR, in the

presence and in the absence of molecular oxygen. As a result, we refined and clarified the mechanism by which RNR inactivation was proposed to occur in an oxidative medium.<sup>19</sup> Additionally, we propose the first reaction path for the chemical events that occur in anaerobiosis and which do not affect RNR activity.

### Theoretical Approach

The theoretical study of the interaction of SHdNDP with the active site residues of RNR was made with the Gaussian 03 program.<sup>21</sup> To perform the study, we used a cutoff of the R1 subunit, composed by a chain of seven amino acid residues (Ser<sub>436</sub>, Asn<sub>437</sub>, Leu<sub>438</sub>, Cys<sub>439</sub>, Leu<sub>440</sub>, Glu<sub>441</sub>, and Ile<sub>442</sub>) plus the side chain of Cys<sub>225</sub>. The inhibitor was modeled without the base, the phosphates, and the C5' carbon atom. Two hydrogen atoms were added to C1' and C4'. The system was composed of a total of 130 atoms.

During geometry optimizations to locate the transition state, the reactants, and the products of the considered reactions, our system was divided into two layers within the ONIOM formalism,<sup>22</sup> as implemented in Gaussian 03. The higher level layer included the inhibitor model and the side chains of Cys<sub>225</sub>, Cys<sub>439</sub>, and Glu<sub>441</sub> in a total of 28 atoms; it was treated with density functional theory (DFT) at the unrestricted B3LYP/6-31G(d) level.<sup>23–25</sup> The rest of the system was treated with the semiempirical method PM3MM.<sup>26</sup> It is important to note that during geometry optimizations the system always kept the conformation of the X-ray crystallographic structure, although no constraints were imposed in the positions of any atom. For each step, we performed a scan of the reaction coordinate with a step value of 0.01 Å and considered the geometry with the higher energy a very good approximation to the geometry of the transition state. From there, we relaxed the system and let it optimize in both directions of the reaction coordinate to obtain the geometries of the respective minima. A single point calculation was then performed on the three stationary points, treating the whole system at the density functional theory level, with the B3LYP functional and the larger 6-31+G(d) basis set. The atomic spin density distributions were calculated with a Mulliken population analysis<sup>27</sup> in the higher level calculation.

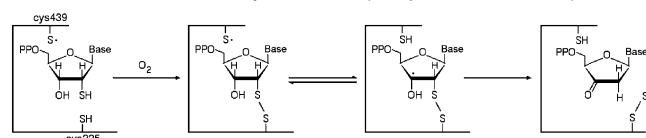
### Results and Discussion

We based ourselves in the available experimental data and in earlier findings about RNR natural catalysis and suicide inhibition, to search plausible mechanistic pathways for RNR

- (11) Stubbe, J.; Ator, M.; Krenitsky, T. *J. Biol. Chem.* **1983**, *258*, 1625.
- (12) Mao, S. S.; Yu, G. X.; Chalfoun, D.; Stubbe, J. *Biochemistry* **1992**, *31*, 9752.
- (13) Lenz, R.; Giese, B. *J. Am. Chem. Soc.* **1997**, *119*, 2784.
- (14) Fernandes, P. A.; Eriksson, L. A.; Ramos, M. J. *Theor. Chem. Acc.* **2002**, *108*, 352.
- (15) Thelander, L.; Larsson, B.; Hobbs, J.; Eckstein, F. *J. Biol. Chem.* **1976**, *251*, 1398.
- (16) Stubbe, J.; Kozarich, J. W. *J. Biol. Chem.* **1980**, *255*, 5511.
- (17) Baker, C. H.; Banzon, J.; Bollinger, J. M.; Stubbe, J.; Samano, V.; Robins, M. J.; Lippert, B.; Jarvi, E.; Resvick, R. *J. Med. Chem.* **1991**, *34*, 1879.
- (18) van der Donk, W. A.; Yu, G.; Silva, D. J.; Stubbe, J.; McCarthy, J. R.; Jarvi, E. T.; Matthews, D. P.; Resvick, R. J.; Wagner, E. *Biochemistry* **1996**, *35*, 8381.
- (19) Covès, J.; de Fallois, L. L. H.; Le Pape, L.; Décout, J.-L.; Fontecave, M. *Biochemistry* **1996**, *35*, 8595.
- (20) Roy, B.; Chambert, S.; Lepoivre, M.; Décout, J.-L. *Nucleosides Nucleotides* **2003**, *22*, 883.

- (21) Frisch, M. J.; Trucks, G. W.; Schlegel, H. B.; Scuseria, G. E.; Robb, M. A.; Cheeseman, J. R.; Montgomery, J. A., Jr.; Vreven, T.; Kudin, K. N.; Burant, J. C.; Millam, J. M.; Iyengar, S. S.; Tomasi, J.; Barone, V.; Mennucci, B.; Cossi, M.; Scalmani, G.; Rega, N.; Petersson, G. A.; Nakatsuji, H.; Hada, M.; Ehara, M.; Toyota, K.; Fukuda, R.; Hasegawa, J.; Ishida, M.; Nakajima, T.; Honda, Y.; Kitao, O.; Nakai, H.; Klene, M.; Li, X.; Knox, J. E.; Hratchian, H. P.; Cross, J. B.; Bakken, V.; Adamo, C.; Jaramillo, J.; Gomperts, R.; Stratmann, R. E.; Yazyev, O.; Austin, A. J.; Cammi, R.; Pomelli, C.; Ochterski, J. W.; Ayala, P. Y.; Morokuma, K.; Voth, G. A.; Salvador, P.; Dannenberg, J. J.; Zakrzewski, V. G.; Dapprich, S.; Daniels, A. D.; Strain, M. C.; Farkas, O.; Malick, D. K.; Rabuck, A. D.; Raghavachari, K.; Foresman, J. B.; Ortiz, J. V.; Cui, Q.; Baboul, A. G.; Clifford, S.; Cioslowski, J.; Stefanov, B. B.; Liu, G.; Liashenko, A.; Piskorz, P.; Komaromi, I.; Martin, R. L.; Fox, D. J.; Keith, T.; Al-Laham, M. A.; Peng, C. Y.; Nanayakkara, A.; Challacombe, M.; Gill, P. M. W.; Johnson, B.; Chen, W.; Wong, M. W.; Gonzalez, C.; Pople, J. A. *Gaussian 03*, revision B.04; Gaussian, Inc.: Pittsburgh, PA, 2003.
- (22) Vreven, T.; Morokuma, K. *J. Comput. Chem.* **2000**, *21*, 1419.
- (23) Becke, A. D. *J. Chem. Phys.* **1993**, *98*, 5648.
- (24) Lee, C. T.; Yang, W. T.; Parr, R. G. *Phys. Rev. B* **1988**, *37*, 785.
- (25) Hertwig, R. W.; Koch, W. *J. Comput. Chem.* **1995**, *16*, 576.
- (26) Stewart, J. J. P. *J. Comput. Chem.* **1989**, *10*, 221.
- (27) Mulliken, R. S. *J. Chem. Phys.* **1955**, *23*, 1833.

**Scheme 2.** Mechanism Previously Proposed by Covès et al. for the Inactivation of RNR by SHdUDP (Adapted from Ref 19)<sup>a</sup>



<sup>a</sup> The base is uracyl.

interaction with SHdNDP. Several possibilities were initially considered, and the ones that were found less favorable, from a kinetic or thermodynamic point of view, were gradually discarded. Schemes 3 and 4 represent the reaction mechanisms that we propose as more viable in the presence and in the absence of molecular oxygen, respectively. Both situations shall now be discussed in detail.

**In the Presence of O<sub>2</sub>.** In experimental studies, Covès et al. found that SHdUDP inhibited purified RNR in a stoichiometric proportion when there was molecular oxygen available in the medium.<sup>19</sup> During inactivation, the loss of the essential tyrosyl radical and the transient formation of a postulated perthiyl radical attached to an active site cysteine was observed. It was proposed that in the presence of O<sub>2</sub> occurred the formation of a disulfide bridge between the 2'-SH group and the SH of Cys<sub>225</sub>. A subsequent homolytic cleavage of the C2'-S bond would generate the perthiyl radical. This mechanism is represented in Scheme 2.

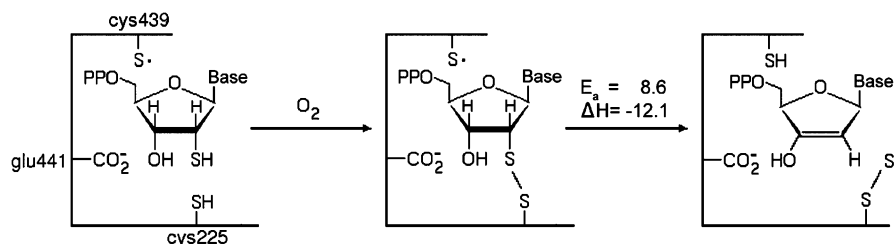
We think that the readily formation of the disulfide bridge between Cys<sub>225</sub> and the inhibitor, in the presence of O<sub>2</sub>, is a very good assumption. In fact, taking into account the redox potentials of the two species, one can conclude that the reduction

of O<sub>2</sub> to water with concomitant oxidation of the SH groups is very favorable. There are three cysteine residues in the RNR active site. Cys<sub>439</sub> is located above the inhibitor ring and cannot interact with its thiol group nor with the other two active site cysteines. Cys<sub>462</sub> is also prevented from interacting with the 2'-SH by the presence of Cys<sub>225</sub> in between. In principle, molecular oxygen could oxidize the Cys<sub>225</sub>-Cys<sub>462</sub> pair to a disulfide, but these cysteines would be readily reduced by the pair Cys<sub>754</sub>-Cys<sub>759</sub>, as it occurs in the natural substrate mechanism. This leaves us with the only reasonable option being the formation of a disulfide bond between the inhibitor and Cys<sub>225</sub>. This disulfide should be prevented from reduction by Cys<sub>754</sub>-Cys<sub>759</sub> due to its different position and orientation when compared to the Cys<sub>225</sub>-Cys<sub>462</sub> disulfide.

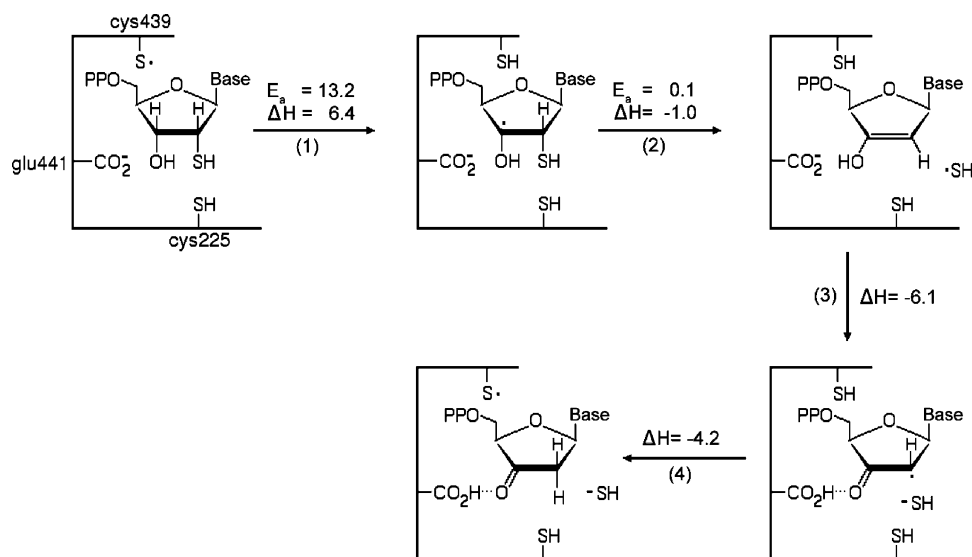
On the basis of these facts, we started the study with a structure where the sulfur atoms of the inhibitor and of Cys<sub>225</sub> were already oxidized to a disulfide and estimated the energetic of the reactions that would follow the sulfur oxidation and lead to the perthiyl radical formation. Our results are summarized in Scheme 3.

The first step of RNR natural catalysis is the abstraction of the 3'-H atom by the radical sulfur of Cys<sub>439</sub>.<sup>12</sup> The same reaction with the SHdNDP disulfide-bonded to Cys<sub>225</sub> is energetically and thermodynamically favorable, having an energetic barrier of 8.6 kcal/mol and a reaction enthalpy of -12.1 kcal/mol. Figure 1 represents the geometry of the transition state. At this point, the 3'-H is halfway between the sulfur and the C3', the C3'-O and C3'-C2' bonds are 0.05 and 0.03 Å shorter than in the reactants, and the C2'-S bond is somewhat elongated.

**Scheme 3.** Proposed Mechanism for RNR Inhibition by SHdNDP; All Energy Values Are in kcal/mol



**Scheme 4.** Proposed Mechanism for the Interaction of SHdNDP with RNR in the Absence of Molecular Oxygen; All Energy Values Are in kcal/mol



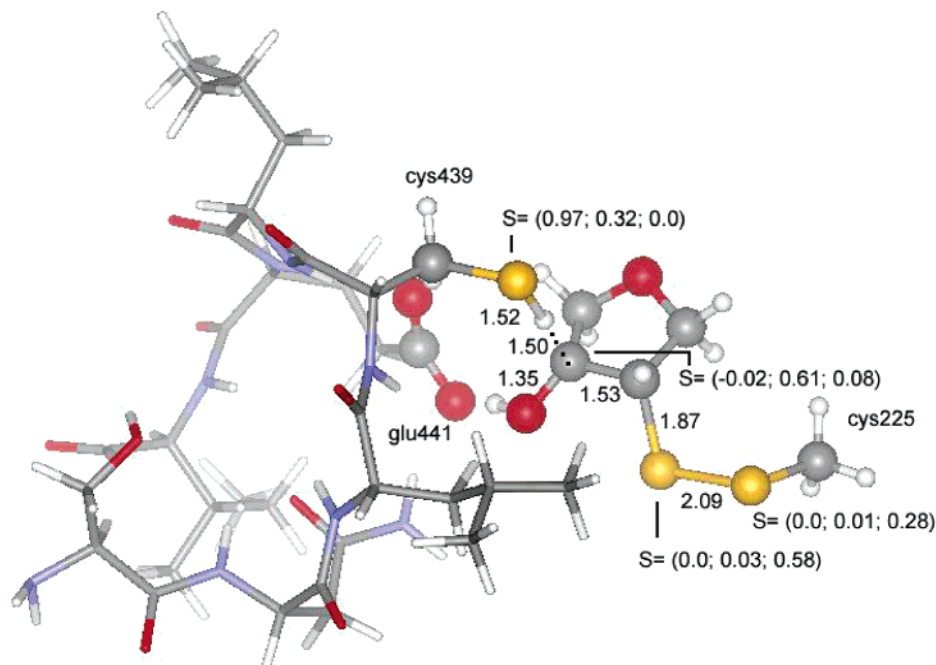


**Figure 1.** Geometry of the transition state labeled with relevant bond lengths (in Å) and the spin density distribution ( $S$ ) in au of the three geometries (reactants, transition state, products, respectively).

During optimization of the products, the sulfur bound to the 2' position detached spontaneously from the carbon, through homolytic cleavage of the C–S bond. Thus, this reaction produces directly the perthiyl radical that had been postulated in the literature to be the one detected transiently during RNR inactivation. In the optimized structure of the products, the C3'–C2' and C3'–O bonds are further shortened to 1.35 and 1.33 Å, respectively, the inhibitor sulfur is 3.35 Å away from C2', and the spin density is in fact concentrated in the two bonded sulfur atoms (0.86 au in total). The spontaneous elimination of a 2' substituent from nucleotide analogues upon 3'-H atom abstraction has been observed before with other RNR mechanism-based inhibitors, e.g. with 2'-azido-2'-deoxyribonucleotides<sup>28</sup> and 2'-chloro-2'-deoxyribonucleotides.<sup>29</sup>

Figure 2 depicts the energetic profile of the reaction that we propose to occur during RNR inactivation by SHdNDP, after the oxidation of the inhibitor's and the Cys<sub>225</sub> thiol groups.

These results give strong support to the proposal that had been made in the literature based solely on experimental work. In fact, our study clarifies the chemical pathway that leads to the transient radical formation and confirms the nature of that radical as being a perthiyl one, which results from an energetically favored reaction. Our proposal deviates from the earlier one in one important aspect: the perthiyl radical is spontaneously formed upon the 3'-H atom abstraction and does not result from an elongated stepwise mechanism. The overall success of this theoretical study in reproducing and refining the experimentally deduced pathway motivated us to use the same models and method in the unraveling of the reaction course that takes place in anaerobiosis.

**In the Absence of O<sub>2</sub>.** From experimental studies, it is known that in the absence of molecular oxygen SHdNDP does not inactivate RNR.<sup>19</sup> If anaerobiosis is maintained for a consider-

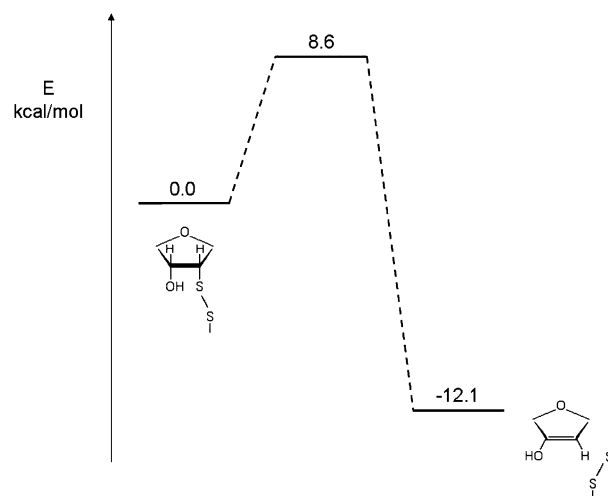


**Figure 2.** Energetics of the proposed mechanism for RNR inhibition by SHdNDP.

able amount of time and then the medium is oxygenated, RNR still remains active. This means that the compound interacts with the enzyme and suffers modifications that lead to the loss of its inhibitory power, otherwise shown in an oxidative medium. The fact that the enzyme modifies the molecule and remains catalytically active led to the suggestion that the reactions involved in the process could match the ones responsible for the reduction of the natural substrates.<sup>19</sup> However, the results of our study indicate important deviations from the natural catalysis. The chemical pathway that we propose to occur in this situation is represented in Scheme 4.

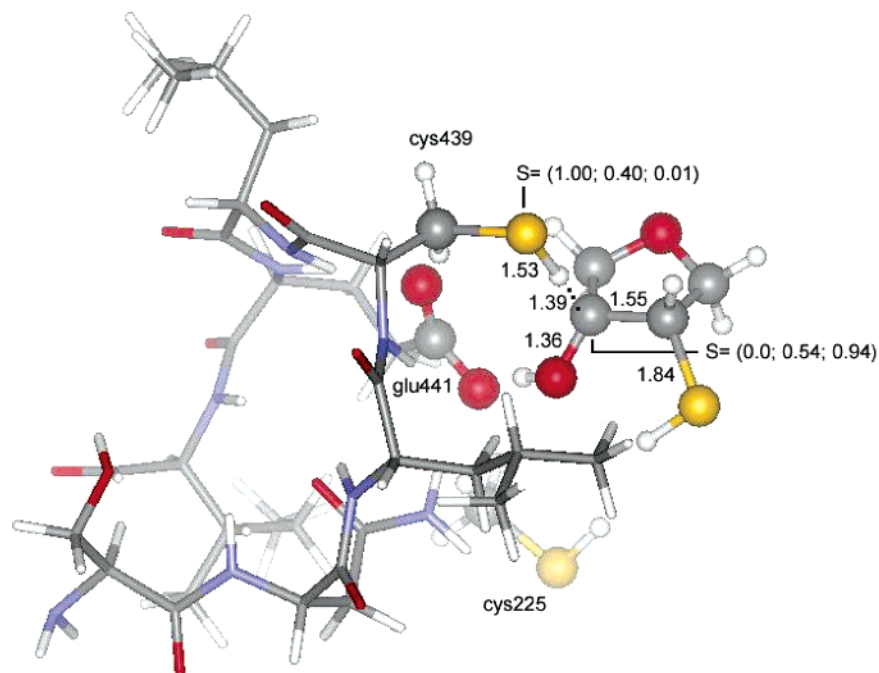
**Reaction 1.** The first step is the abstraction of the 3'-H atom by the radical sulfur of Cys<sub>439</sub>, just as it is known to happen in normal catalysis. The activation energy for this reaction is 13.2 kcal/mol, and the reaction enthalpy is 6.4 kcal/mol.

Figure 3 depicts the geometry of the transition state, where the 3'-H atom is 1.53 Å away from the sulfur and 1.39 Å from

(28) Pereira, S.; Fernandes, P. A.; Ramos, M. J. *J. Comput. Chem.* **2004**, *25*, 227.

(29) Fernandes, P. A.; Ramos, M. J. *Chem.-Eur. J.* **2003**, *9*, 5916.





**Figure 3.** Geometry of the transition state for reaction 1, labeled with relevant bond lengths (in Å) and the spin density distribution ( $S$ ) in au of the three geometries (reactants, transition state, products, respectively).

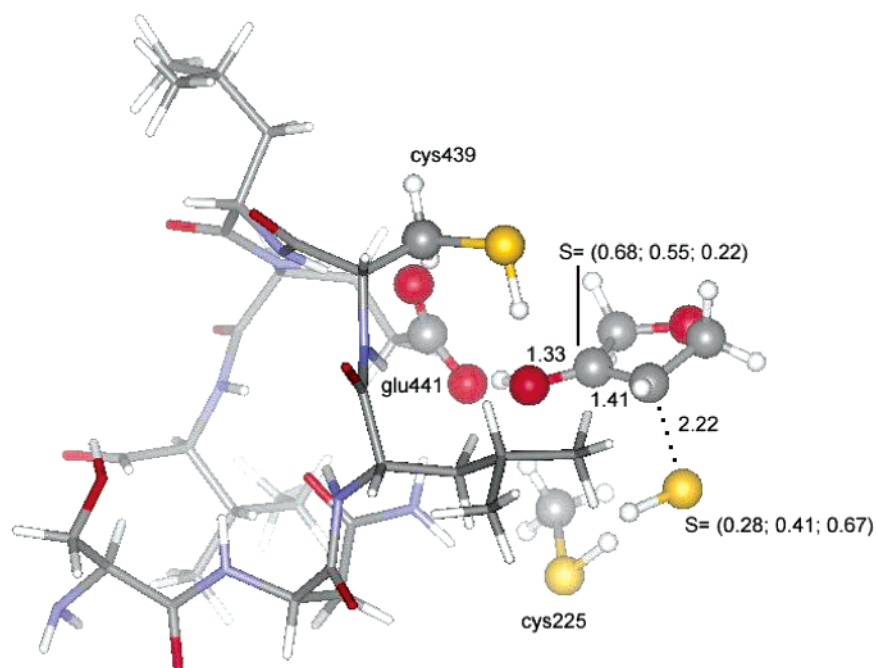


**Figure 4.** Geometry of the transition state for reaction 2, labeled with relevant bond lengths (in Å) and the spin density distribution ( $S$ ) in au of the three geometries (reactants, transition state, products, respectively).

the carbon C3'. The C3'–O bond is 0.05 Å shorter than in the reactants (1.41 to 1.36 Å), and the hydrogen bond with Glu<sub>441</sub> is also shorter by 0.13 Å (1.75 to 1.62 Å). The spin density is no longer concentrated in the Cys<sub>439</sub> sulfur but is now largely delocalized to the carbon C3'.

In the products, the C3'–C2' and C3'–O bonds are shortened to 1.47 and 1.34 Å, respectively, and the C2'–S bond is elongated to 1.96 Å. The spin density is concentrated in the C3' atom.

**Reaction 2.** At the end of reaction 1, the C2'–S bond has been elongated to 1.96 Å, which is evidence that this bond can be easily broken. Indeed, we found that such reaction was almost

spontaneous, with a vanishing barrier of 0.1 kcal/mol and an enthalpy of reaction of  $-1.0$  kcal/mol.

The transition state for reaction 2 is represented in Figure 4. At this point, the C2'–S bond is further elongated to 2.22 Å and the spin density is almost equally shared by these two atoms, indicating a homolytic cleavage of the covalent bond.

In the optimized structure of the products, the sulfur atom is 2.75 Å away from the carbon C2' and the C2'–C3' bond is 0.07 Å shorter than in the reactants (1.44 to 1.37 Å); the spin density is mainly located at the sulfur although it is still delocalized to the carbon C3'.

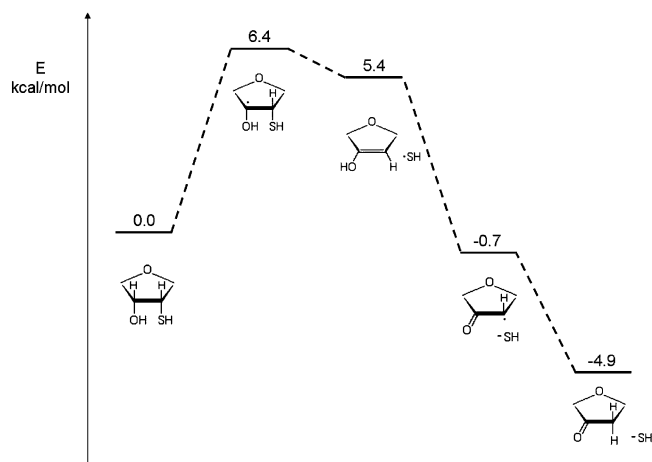


**Figure 5.** Energetic profile of the mechanism proposed for the RNR interaction with SHdNDP in the absence of molecular oxygen.

The elimination of the SH group is an important deviation from the natural substrate mechanistic pathway. In the natural catalysis, the 2'-OH group is protonated by Cys<sub>225</sub> and leaves the ribose in the form of a water molecule. Here, the protonation of the thiol group is not thermodynamically favored.

**Reaction 3.** The third reaction consists of the transfer of a proton from the 3'-O atom to the glutamate residue glu441. This rearrangement of the system is thermodynamically favorable, with a  $\Delta H$  of  $-6.1$  kcal/mol, and leads to the formation of a radical ribose-derived furanone. As a result, the negative charge of the system becomes mainly localized in the SH group (0.63 au), and the spin density becomes delocalized between the carbon C2' (0.53 au), the 3'-O atom (0.17 au), and the sulfur of the thiol group (0.27 au).

**Reaction 4.** It is experimentally known that the protein radical is regenerated in anaerobic conditions.<sup>19</sup> At this point of the reaction pathway, there is clearly one step that would lead to that regeneration. It consists of the donation of the thiol hydrogen atom of Cys<sub>439</sub> to the carbon C2'. As a consequence, the initial thiyl radical is regenerated and the enzyme is ready for another catalytic turnover. This mechanistic step has been proposed before to occur with other nucleotide analogues at the active site of RNR, e.g. with 2'-chloro-2'-deoxyribonucleotides<sup>29</sup> and 2',2'-difluoro-2'-deoxyribonucleotides.<sup>30</sup>

We found the step to be thermodynamically favorable with an enthalpy of reaction of  $-4.2$  kcal/mol. In the products, the spin density is, in fact, concentrated in the cys439 sulfur atom (0.87 au) and is only slightly delocalized to the sulfur of the thiol group (0.11 au); the negative charge of the system is still mainly located in the SH group ( $-0.62$  au). The C3'-O bond is 0.05 Å shorter (1.27 to 1.22 Å) and the C3'-C2' bond is 0.11 Å longer (1.40 to 1.51 Å) than in the reactants, which reflects the formation of a ketone.

This reaction pathway is similar to the RNR inhibition mechanism by 2'-chloro-2'-deoxyribonucleotide.<sup>29,31</sup> The chloride also leaves spontaneously the ring in the ionic form, and the tyrosyl radical is regenerated through the donation of an H atom by cys439 to the C2' carbon. In that case, RNR becomes inactivated when the newly formed ketone leaves the active site,

loses the base and the phosphates in solution, and interacts with external residues of R1. The interaction is detected by the formation of a characteristic chromophore with absorption at 320 nm and is prevented by the existence of reductive species in solution, which intercept the furanone. In the studies with SHdNDP, the detection of the chromophore was not reported, but its formation cannot be discarded as all experiments were performed with reductants present in the medium.

In Figure 5, we present the energetic profile of this mechanistic pathway. It has an overall reaction energy of  $-4.9$  kcal/mol and is therefore thermodynamically favored, especially if we consider the easy escape of the thiolate group from the active site and its solvation in the aqueous solvent.

## Conclusion

A theoretical study was conducted on the interaction of RNR with SHdNDP, in the absence and in the presence of molecular oxygen. The calculations to model the chemical events in the presence of O<sub>2</sub> were made assuming the prompt formation of a disulfide bridge between the thiol groups of the inhibitor and of Cys<sub>225</sub>. This was proposed in the literature as a plausible way to form the transient radical, which was detected in *in vitro* experiments and postulated to be a perthiyl one.<sup>19</sup>

As a result of this work, we propose a refined proposal for the reaction path in aerobiosis and the first mechanistic pathway for the interaction of SHdNDP with RNR in anaerobiosis.

In both situations, the first step is the 3'-H atom abstraction by the radical sulfur of Cys<sub>439</sub> with subsequent cleavage of the C2'-S bond.

In anaerobiosis, the second step produces an SH group that remains interacting with the ribose in a radical-anionic/keto-enolic equilibrium. Cys<sub>439</sub> then donates an H-atom to the C2' carbon, regenerating the initial thiyl radical. A ribose-derived furanone is formed, and the SH group leaves the active site in the anionic form. The furanone that constitutes the end-product of the mechanism is known to inhibit subunit R1, producing a chromophore with a characteristic absorption at 320 nm, but this interaction is prevented by the presence of reductants in solution. Thus, the nondetection of the chromophore in the experimental studies performed with SHdNDP and the fact that RNR remains active can be explained by the existence of reductive species in all of the experiments.

In the presence of O<sub>2</sub>, the C2'-S cleavage is spontaneous and produces the perthiyl radical Cys<sub>225</sub>-S-S· that was proposed to be the one detected experimentally. The thiyl radical is not regenerated, and subunit R2 becomes inactivated. Subunit R1 was found to remain active, which suggests that Cys<sub>225</sub> will be reduced by the enzymatic machinery as happens with the disulfide bridge formed in the natural catalysis between this cysteine and Cys<sub>462</sub>. The proposed mechanistic pathway is in agreement with the earlier experimental proposal, contributing to a clarification and detailing of the elementary chemical steps.

**Acknowledgment.** We thank the FCT (Fundação para a Ciência e Tecnologia) for a doctoral scholarship for S.P. and for financial support (Projecto Pocti/35736/99, Portugal), and the NFCR (National Foundation for Cancer Research) Centre for Drug Discovery, University of Oxford, UK.

**Supporting Information Available:** Cartesian coordinates of all of the stationary points discussed. This material is available free of charge via the Internet at <http://pubs.acs.org>.

JA046662W

(30) Pereira, S.; Fernandes, P. A.; Ramos, M. J. *J. Comput. Chem.* **2004**, *25*, 1286.

(31) Ator, M. A.; Stubbe, J. *Biochemistry* **1985**, *24*, 7214.